



# Fabrication of Porous Silicon as a Gas Sensor: The Role of Porous Silicon Surface Morphology

Ahmed Z. Abdullah, Adawiya J. Haider\*, Allaa A. Jabbaar

Department of Applied Sciences, University of Technology – Iraq

## Article information

### Article history:

Received: January, 27, 2022

Accepted: April, 15, 2022

Available online: December, 10, 2022

### Keywords:

Laser-assisted,  
Etching,  
Porous silicon,  
Surface area,  
Pollutant gases sensor

### \*Corresponding Author:

Adawiya J. Haider

[adawiya.j.haider@uotechnology.edu.iq](mailto:adawiya.j.haider@uotechnology.edu.iq)

## Abstract

Manufacture of an environmental polluting gas sensor with improved properties by controlling the preparation conditions of the photo-electrochemical etching technique (PECE). The amount of porosity, the diameter of the pores, and the thickness of the prepared layer of porous silicon (PSi) can be controlled by changing one or all of these conditions. In this paper, n-type Si with a crystalline orientation (100) was used, whereby PSi was prepared with the use of a red diode laser with a wavelength of 650 nm, using different radiation intensity, and with the constancy of etching time and current density. Through the results obtained, it was noted that: the porosity increases significantly up to 75% as well as the thickness of the PSi layer up to 1.45  $\mu\text{m}$  with the increase in the intensity of the laser beam. Also, examining the morphology of the surface samples by field emission scanning electron microscope (FE-SEM) besides, the average pore diameters of the prepared samples were calculated. It is clear that the intensity of the laser beam used in the irradiation process is one of the important factors in determining the properties of the prepared PSi. PSi samples have been tested by FTIR to investigate chemical bonds on surfaces such as, (Si-Si, Si-H, Si-H<sub>2</sub>, Si-O-Si, Si-O-Si, Si-H, Si-O-Si). Samples tested as gas sensors and noticed that an increase in the sensing current to 5.3  $\mu\text{A}$  has appeared with the increase of porosity value where methanol gas is used as background.

DOI: [10.53293/jasn.2022.4661.1134](https://doi.org/10.53293/jasn.2022.4661.1134), Department of Applied Sciences, University of Technology

This is an open access article under the CC BY 4.0 License.

## 1. Introduction

The unusual physical and optical features of porous silicon (PSi) have attracted a lot of attention from researchers in recent years. It has a wide range of applications in a variety of technology disciplines, including optical electronics, sensors, medical, and other fields of study. [1, 2]. These features are the result of an increase in the surface area about the volume, or, to put it another way, an increase in the number of pores per unit volume, as the surface area increases. It is possible to produce PSi in a variety of ways, including by the use of metals, wet methods, galvanic methods, and electrostatic methods. [3, 4].

## 2. Theoretical Part

PSi can be prepared in a cost-effective, easy, and efficient manner using these approaches. As a result of the addition of new attractive characteristics to the PSi created using one of the ways, [5]. Typically, the area available or exposed to the target gases is the biggest in efficient gaseous sensors. This is due in part to the target gas (absorbed by the area exposed to the gas) interacting with the PSi, modifying the PSi's electrical and optical properties. [6]. To enhance the PSi surface area exposed to the gas, the percentage number of pores and roughness of the nanostructures must be increased. As a result, the sensor will be more efficient. [7, 8]. In the present work, a PECE technique was used. This method consists of an electrical cell with electrodes, the negative electrode of platinum, Pt has been used because of its high chemical resistance, is connected to the negative part of the electric source, and the anode is connected to the positive electrode of the electric current source and this electrode is made of silicon to be prepared as PSi. When putting n-type with orientation (100) silicon inside the container, it is connected to the anode, and this causes the wafer to be reverse biased, so the laser is used to generate a pair (electron-hole) on the surface of the water, which leads to the passage of current through it and the start of the reaction process. PECE technique is a suitable technique for preparing n-type PSi [9, 5]. The porosity has a great influence in determining the application used for PSi, each porosity has its application [10, 4]. The amount of porosity of the samples prepared in this way depends on several parameters, the most important of which are the concentration of the solution, the current density, the etching time, and the intensity of the laser beam applied to the sample [11-13]. The influence of laser beam intensity on the amount of porosity and pore diameter of the sample prepared from n-type silicon has been studied in this work, as has the latter's effect on the amount of sensitivity, which has been discussed with the usage of methanol gas [14, 15]. When used as a sensor for environmental pollution with toxic gases, the PSi was prepared and studied to determine the effect of the preparation conditions on its properties [16, 17].

### 3. Experimental Procedure

In Figure 1, the conventional cell diagram required for PECE is shown, where n-type silicon with a crystalline direction of (100) is used. Si wafer is placed in the cell after the cleaning process and linked as shown in Figure 1. In this process, a 650-nm red color diode laser is used to achieve the greatest penetration depth of silicon to produce a thick layer of PSi if a short wavelength laser was used [18-19] where the maximum power of the diode laser is 100mw.

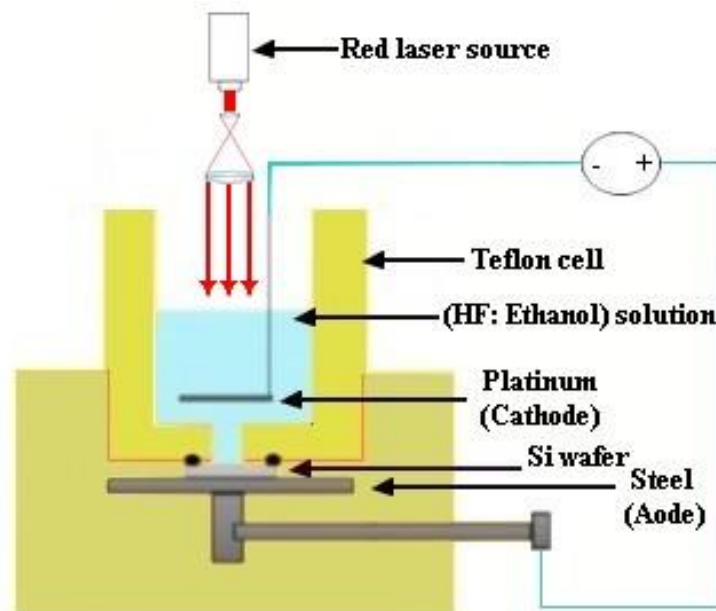


**Figure 1:** The Schematic drawing of the PECE technique.

The current density was fixed at  $8 \text{ mA/cm}^2$  and during 20 min, different laser intensities ( $10, 15, 20, 25 \text{ mw/cm}^2$ ) is changed and after the completion of the etching process, the amount of porosity ( $p$ ) is calculated for each sample according to the following weight equation [20] :

$$P\% = \frac{m_1 - m_2}{m_1 - m_3} \quad (1)$$

Where  $m_1$  is the weight before the etching process,  $m_2$  is the weight after the etching process and  $m_3$  is the weight of the sample after removing the porous layer, using a (NaOH) solution, and is shaken for 20 min to remove the formed PSi layer [21]. After calculating the percentage of porosity, the effect of the intensity of the laser beam on the thickness of the PSi layer can be calculated through the following equation [22]:

$$d = \frac{m_1 - m_3}{A \rho} \quad (2)$$

Where ( $d$ ) is the thickness of PSi, ( $A$ ) is the area of PSI that is exposed to irradiance, ( $\rho$ ) is the density of silicon is about 2.3 gm/cm<sup>3</sup>. Field Emission scanning electron microscopy (FE-SEM) was used to investigate the surface morphology of porous silicon. (Per Kin –Elmer spectrometer) was used for the Fourier transfer infrared (FTIR) spectrometer studies. Finally, the sensitivity current was measured in a methanol atmosphere using a locally-made system.

## 4. Results and Discussion

### 4.1. Morphology of PSi Layer (porosity & layer thickness)

Porosity, porous layer thickness, and surface topography dependent on the etching conditions are the most significant morphological factors of the PSi layer. Through the calculation of the porosity of the sample according to Eq. (1) above, we note the relationship between the intensity of the laser radiation and the amount of porosity is a growing relationship as shown in Figure 2. Where the increase in the porosity was observed with the increase of the laser intensity. This is consistent with the research [8, 23]. In addition to that, the thickness of the porous layer is calculated in different laser intensities according to Eq. (2). Through the results that were reached and according to the graph in Figure 3, it was observed that the thickness of the PSi layer increases with the increase in the intensity of the laser beam and this is consistent with the research of S. Polisski et al. [19]. This indicates that the laser intensity parameter has a significant impact in determining the thickness of the PSi layer.

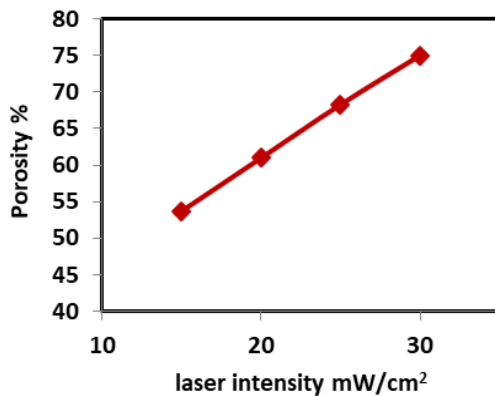


**Figure 2:** Porosity vs etching laser intensity.

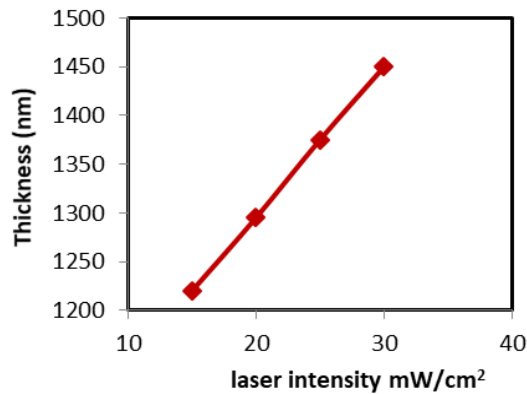


**Figure 3:** layer thickness vs etching laser intensity.

Figure 4 shows four images of the PSi that have been prepared with different values of the intensity of the laser 10, 15, 20, and 25 mW/cm<sup>2</sup>. On the other hand, it can be seen the effect of the intensity of the laser beam on the diameter of the pores produced during the etching process is illustrated in Figure 4. Where the increase in the diameter of the pores resulting from the increase in the intensity of the laser beam was observed, and this is consistent with the research [22]. Figure 4(a) illustrated that the pores size of the porous layer was estimated in the range (250-1000 nm) at etching laser intensity equal to 10 mW/cm<sup>2</sup>, and the high percentage of pores numbers was at 850 nm. We can note here a wide distribution range of pores sizes with silicon structures surrounding the pores (walls) of approximately 500-700 nm, as these regions are considered ineffective as gas absorption regions. When the laser intensity is increased to 15 mW/cm<sup>2</sup> as shown in Figure 4(b), the silicon

dissolution process will increase and thus increase the electron-hole pair generation [8]. The PSi layer appears with a pore diameter ranging from 200 to 700 nm and a maximum percentage number of this pore size reaching 500 nm. It can be observed a formation of the second gradation in a formation of the porous layer leads to an increase in the surface area of the PSi layer, and thus increases the area exposed to the gas [19]. Another thing that contributes to the effectiveness of the area exposed to the gas and the increase in the efficiency of the silicon sensor is the apparent roughness in the surface and the smallness of the silicon nanostructures (pores walls). When using a laser intensity that ranged from 20-25 mW/cm<sup>2</sup> as in Figures 4c and 4d. We notice that the increase in the silicon dissolution process has reached its peak so that it becomes an overlap between the small pores to produce pores with a diameter of between 1-5  $\mu$ m. As well as increasing the sizes of silicon nanostructures, which leads to a decrease in the surface area of the PSi surface, where we exclude the use of these surfaces as gas sensors.

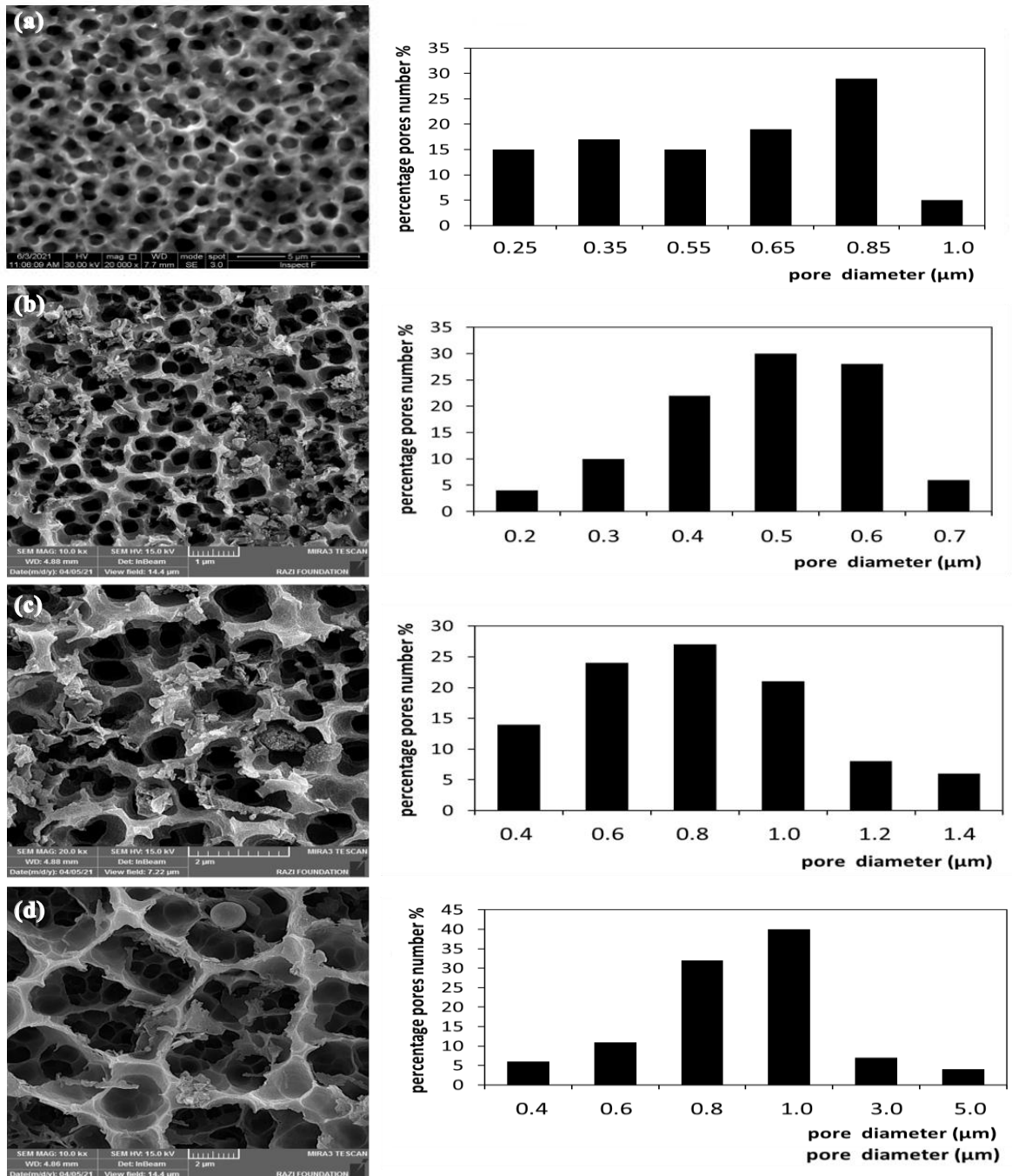


**Figure 4:** Illustrates the morphology and statistical distributions of samples that are prepared in different laser intensities; a) 10, b) 15, c) 20, and d) 25  $\text{mw}/\text{cm}^2$ , all samples etched with a current density of 8  $\text{mA}/\text{cm}^2$  and during 20 min.

#### 4.2. Fourier-transform infrared spectroscopy (FTIR) Analysis

Considering that the FTIR study is perhaps one of the most powerful tools for determining the types of functional groups (chemical bonds) on surfaces, this technique was used to find out these bonds on the PSi surface. The Characterization of chemical species on PSi layers has been done. The FTIR signals from (high surface area) PSi were stronger compared to the signals obtained from the (low surface area) PSi. The hydrogen bonds are a result of the etching process, so the  $\text{Si-H}_x$  silane groups ( $x=1, 2$ , and 3) were formed on the surface of the PSi layers. The type of  $\text{Si-H}_x$  silane groups (1, 2, and 3) undergo a surface morphology consistent with the results of [8, 23, 24]. The absorption band intensity (FTIR) was correlated with the vibrational pattern of the (H) chemical bond, then the range used to absorb PSi was from  $400\text{--}1500\text{cm}^{-1}$ . Figure 5 illustrates FTIR absorption spectra as a function of (etching power density) which are (10, 15, 20, and 25)  $\text{mw}/\text{cm}^2$ . The spectra contained monohydride ( $\text{Si-H}$ ) bonds, di-hydride ( $\text{Si-H}_2$ ) bonds, and tri-hydride ( $\text{Si-H}_3$ ) bonds.

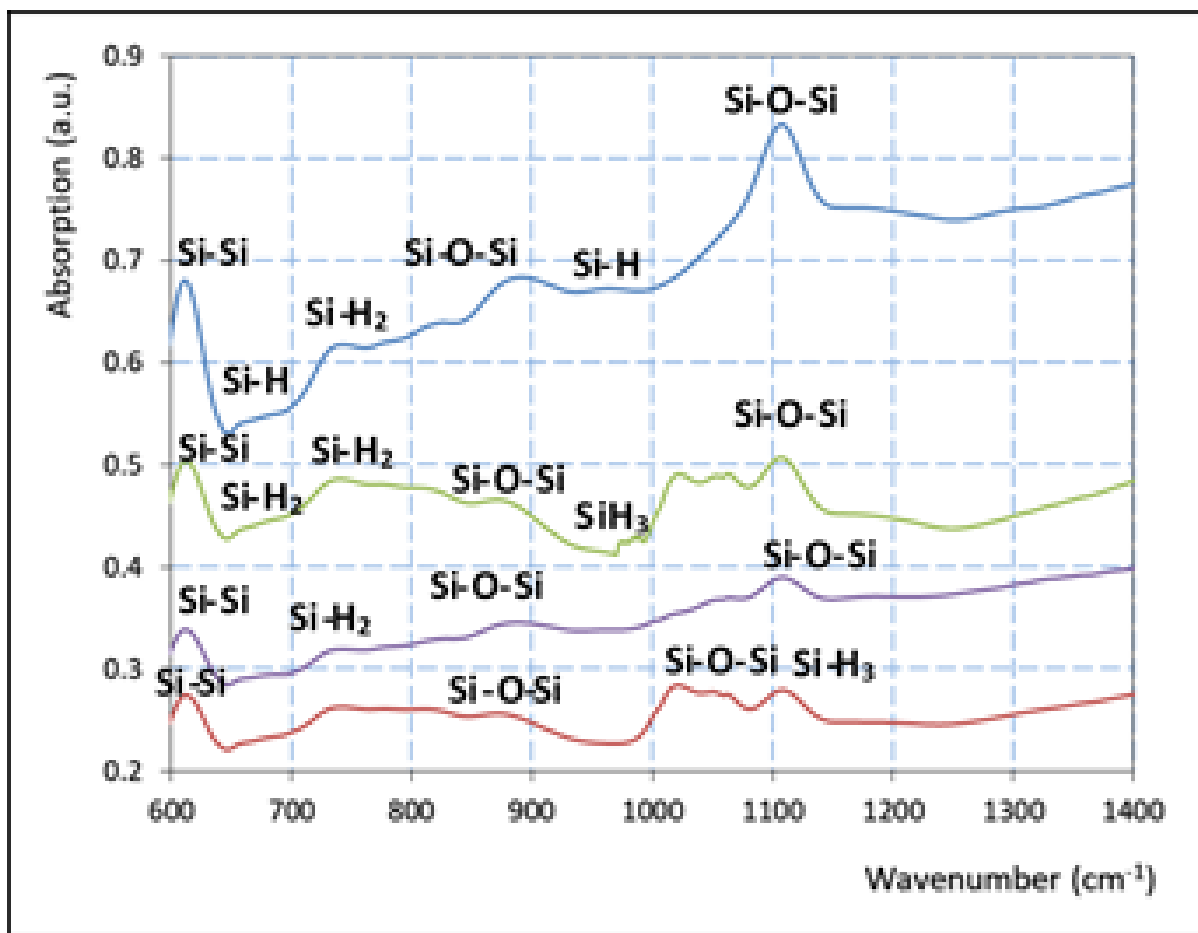


**Figure 5:** FTIR absorption spectra of PSi prepared in different laser intensity; a) 10  $\text{mw}/\text{cm}^2$ , b) 15  $\text{mw}/\text{cm}^2$ , c) 20  $\text{mw}/\text{cm}^2$  and d) 25  $\text{mw}/\text{cm}^2$

The intensity of the absorption due to the di-hydride ( $\text{Si-H}_2$ ) and the tri-hydride ( $\text{Si-H}_3$ ) increased with increasing etching power density. The morality was stated in fact that with increasing surface area of the PSi layer, the crystallized silicon within the porous structure becomes smaller and changes the nature of the surface. Peak absorption variance and associated wave number as a function of etching power density are tabulated in Table 1. Therefore, the density (amount) of bonded hydrogen and consequently the absorption increased with an increase of the surface area of the PSi layer in the same way as the absorption increased due to the termination of  $\text{Si-O-Si}$  with an increase of the porosity. Thus, the PSi surface layer, which is prepared with 15  $\text{mW}/\text{cm}^2$  etching

power density at a constant current density of 8 mA/ cm<sup>2</sup> and during 20 min has higher absorption peak intensity, especially for the CH<sub>3</sub>, Si-O-Si, Si-H<sub>2</sub> chemical bonds.

**Table 1:** Peak position of chemical bonds of the prepared PSi with different laser intensities; a)10, b)15, c) 20, and d) 25 mw/cm<sup>2</sup> at a fixed etching current of about 8 mA/cm<sup>2</sup> 8 and with etching time of 20 min.

Power density mW/ cm <sup>2</sup>	Peak of absorption red	Chemical bonds	Wave number cm <sup>-1</sup>
10	0.67	Si-Si	615
	0.54	Si-H	661
	0.61	Si-H <sub>2</sub>	740
	0.63	Si-O-Si	852
	0.68	Si-O-Si	887
	0.67	Si-H	966
	0.82	Si-O-Si	1112
15	0.49	Si-Si	615
	0.43	Si-H <sub>2</sub>	659
	0.48	Si-H <sub>2</sub>	742
	0.47	Si-O-Si	823
	0.46	Si-O-Si	881
	0.48	CH <sub>3</sub>	989
	0.50	Si-O-Si	1112
20	0.33	Si-Si	615
	0.29	Si-H <sub>2</sub>	659
	0.31	Si-H <sub>2</sub>	734
	0.32	Si-O-Si	823
	0.34	Si-O-Si	891
	0.38	Si-O-Si	1116
25	0.25	Si-Si	615
	0.21	Si-H <sub>2</sub>	659
	0.26	Si-H <sub>2</sub>	740
	0.25	Si-O-Si	819
	0.28	Si-H <sub>3</sub>	1026
	0.27	Si-O-Si	1114

#### 4.3. Sensing current of PSi samples

Figure 6 shows the amount of the sensing current relative to the time, the sensor was exposed to a specific amount of methanol, where four PSi sensors were examined respectively (a, b, c, d), each sensor was prepared with a different laser intensity (10, 15, 20, 25) mw/ cm<sup>2</sup> respectively.

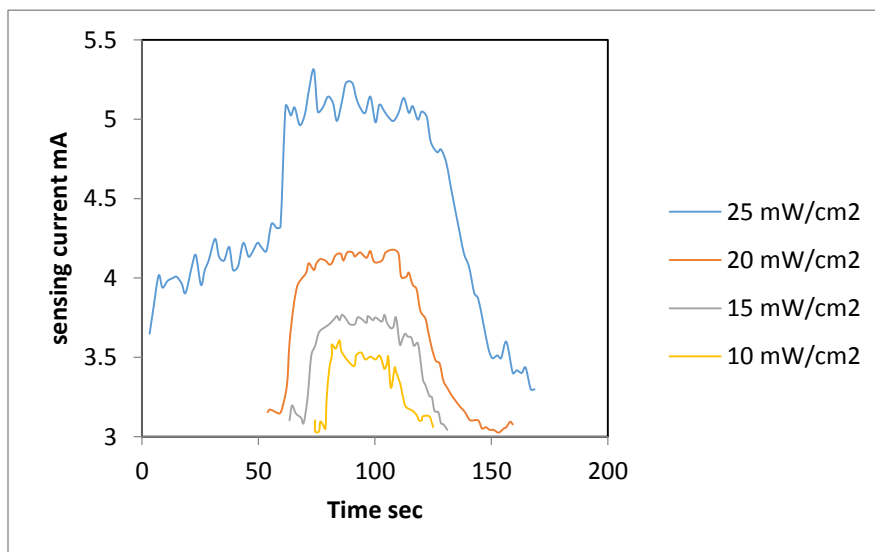


**Figure 6:** Illustrated the sensing current to exposure time for different power densities (10, 15, 20, 25)  $\text{mW}/\text{cm}^2$ . Where it was found that the highest sensitization current is for sample B, which has the highest porosity, then sample C, which has a lower porosity than the previous sample, and then sample D, and then the least sensitivity is the share of sample A, which has the lowest porosity. As the sensor having less porosity leads to having the least surface area (poor capturing for gas molecules) and this is consistent with the research of [25], where sensitivity to reagents is effectively linked to the surface area, meaning that increasing the surface area leads to an increase in the sensitivity current. The impact of the laser intensity on the amount of porosity and therefore the surface area of the sensor is what regulates the degree of sensitivity, as shown in Figure 6.

#### 4. Conclusions

It was discovered in the work that the etching laser intensity played a significant role in changing the properties of the formed PSi layer; when the laser intensity was increased to its maximum, the porosity and layer thickness of the formed PSi layer increased to greater heights, resulting in an increase in the surface area of the formed PSi layer and the formation of new effective chemical bonds in the porous layer, as shown in the results. Optimization of the laser parameters and acid percentages utilized in the etching process, together with a consistent etching duration and etching current, demonstrated the controllability of the shape and properties of the PSi surface. Finally, due to the higher capture of gas particles evaluated for the PSi sensor, an increase in the sensing current to 5.3 A was observed.

#### Acknowledgment

The authors gratefully acknowledge the financial and technical support provided by the Applied Sciences Department, University of Technology-Iraq.

#### Conflict of Interest

The authors declare no conflict of interest.

#### References

- [1] S. K. Abdulridha, S. A. Tuma and O. A. Abdulrazzaq, "Study of the Partial Shading Effect on the Performance of Silicon PV Panels String," *Journal of Applied Sciences and Nanotechnology*, Vol. 1, pp. 32-42, 2021.
- [2] M. A. Al-Kinani, A. J. Haider and S. Al-Musawi, "Study the Effect of Laser Wavelength on Polymeric Metallic Nanocarrier Synthesis for Curcumin Delivery in Prostate Cancer Therapy: In Vitro Study," *Journal of Applied Sciences and Nanotechnology*, Vol. 1, pp. 43-50, 2021.
- [3] K. H. Jawad and B. Hasson, "Developing Strategy for a Successful Antioxidant, Anticancer Activity via an Improved Method Prepared to Porous Silicon Nanoparticles," *Journal of Applied Sciences and Nanotechnology*, Vol. 1, Issue 4, pp. 1-11, 2021.
- [4] A. J. Haider, "the effect of some experimental parameters on the properties of porous silicon," *Iraqi J. of appl. Phys.*, vol. 4, pp. 37-40, 2008.
- [5] L. Koker and Kurt W. Kolasinski, "Photoelectrochemical etching of Si and porous Si in aqueous HF," *Phys. Chem. Chem. Phys.*, Vol. 2, pp. 277-281, 2000.
- [6] F. A. Harraz, A. A. Ismail, H. Bouzid, S.A. Al-Sayari, et al., "Surfactant-enhanced Raman scattering (SERS)-active substrates from silver plated-porous silicon for detection of crystal violet," *Applied Surface Science*, Vol. 331, pp. 241-247, 2015.
- [7] A.A. Salih, A. J. Haider and A. Nazar, "Preparation and Characterizations of Nanomaterial by Pulsed Laser Ablation in Liquid (PLAIL) as Friendly Environment Paint," *Journal of Physics: Conference Series*, Vol. 1795, 2021.
- [8] A. J. Haider, A. D.Thamir, A. A. Najim & G. A. Ali, "Structural, morphological and optical properties of  $\text{LiCo}_0.5\text{Ni}_0.45\text{Ag}_0.05\text{O}_2$  thin films" *Plasmonic*, vol.11, no.2-A, pp.351-696,2016.

- [9] A. D. Thamir, A. J. Haider, G. A. Ali, "Preparation of Nanostructure TiO<sub>2</sub> at Different Temperatures by Pulsed Laser Deposition as Solar Cell, Engineering and Technology Journal, Vol. 34, issue.2 part (A) pp. 193-204, 2016.
- [10] S. Ossicini, L. Pavesi and F. Priolo, "Light Emitting Silicon for Microphotonics," Springer-Verlag Berlin Heidelberg, 2003.
- [11] F. A. Fadhil, F. I. Sultan, A. J. Haider "Preparation of poison gas sensor from WO<sub>3</sub> nanostructure by pulsed laser deposition", IOP Conference Series: Materials Science and Engineering, Vol. 2190, 2019.
- [12] E. M. Abdeirazek, A. M. Alwan, M. Kamal, et al., "Spectroscopic aspects of gradient-porosity system," IJESRT, Vol. 3, pp.298-306, 2014.
- [13] A. J. Haider, R. M. Alhaddad, K. Z. Yahya, "Nanostructure dopants TiO<sub>2</sub> films for gas sensing," Iraqi Journal of Applied Physics, Vol. 7, no.2 pp. 27-31, 2011.
- [14] F. Ramírez-González, G. García-Salgado, Enrique Rosendo, Tomás Díaz, Fabiola Nieto-Caballero et al, "Porous Silicon Gas Sensors: The Role of the Layer Thickness and the Silicon Conductivity" Sensors, vol. 20, 2020.
- [15] R. A. Abbas and Doha Adil Abbas, "Theoretical Study and Modeling of Porous Silicon Gas Sensors" Iraqi Journal of Science, Special Issue, pp: 84-90, 2019.
- [16] M. M. Arafat, et al "Gas sensors based on one dimensional nanostructured metal-oxides: A Review", Sensors, Vol. 12, pp. 7207–7258, (2012).
- [17] A. J. Haider and F. I. Sultan, "Structural, morphological and random laser action for dye-ZnO nanoparticles in polymer films". International Journal of Nanoelectronics and Materials, vol.11, pp. 97-12, 2018.
- [18] A. J. Haider, H. A. Mutasher, "A Study on the Structural, Optical and Electrical Properties of Tungsten Trioxide WO<sub>3</sub> Thin Film for Gas Sensing Applications," Engineering and Technology Journal, Vol. 33, issue, 8 part (B) pp. 1473- 1482, 2015.
- [19] A. J. Haider, Riyadh Al-Anbari, Hiba M Sami, Mohammed J Haider, Enhance preparation and characterization of nickel-oxide as self-cleaning surfaces," Energy Procedia, vol. 157, PP.1328-1342, 2019
- [20] Z. C. Feng and R. Tsu, "Porous silicon," World scientific, London (1994).
- [21] S. K. Saxena, V. Kumar, H. M. Rai, et al., "Study of porous silicon prepared using metal-induced etching (MIE): a comparison with laser-induced etching (LIE)," Silicon, Vol. 1, pp. 1-6, 2015.
- [22] S. Polisski, B. Goller, A. Lapkin, et al, "Synthesis and catalytic activity of hybrid metal/silicon nanocomposites," physica status solidi (RRL)-Rapid Research Letters, vol. 2, pp. 132-134, 2008.
- [23] A. Haider, R. Al-Anbari, G. Kadhim, Z. Jameel "Synthesis and photocatalytic activity for TiO<sub>2</sub> nanoparticles as air purification", MATEC Web of Conferences, 2018.
- [24] P. Gupta, A. C. Dillon, A. S. Bracker and S.M. George, "FTIR studies of H<sub>2</sub>O and D<sub>2</sub>O decomposition on porous silicon surfaces," Surface Science, Vol. 245, pp. 360-372, 1991.
- [25] G. F. Fine, L. M. Cavanagh, A. Afonja, et al, "Metal oxide semi-conductor gas sensors in environmental monitoring," Sensors, Vol. 10, pp. 5469–5502, 2010.